Available online at www.sciencedirect.com
SCIENCE DIRECT®
Sensors and Actuators A 110 (2004) 395–400
SENSORS AND ACTUATORS A PHYSICAL
www.elsevier.com/locate/sna

Technological aspects on the fabrication of silicon-based optical accelerometer with ARROW structures

A. Llobera [a,*], J.A. Plaza [a], I. Salinas [b], J. Berganzo [c], J. Garcia [c], J. Esteve [a], C. Domínguez [a]

[a] IMB-CSIC, Campus UAB, Cerdanyola, Barcelona 08193, Spain
[b] Instituto de Investigación en Ingeniería de Aragón I3A, Universidad de Zaragoza, Zaragoza, Spain
[c] Departamento de Electrónica y Componentes, Ikerlan, Gipuzkoa, Spain

Received 20 September 2003; received in revised form 15 October 2003; accepted 24 October 2003

Abstract

The fabrication and characterization of an optical accelerometer based on silicon technology and using BESOI wafers is presented. Instead of the standard total internal reflection (TIR) waveguides, AntiResonant Reflecting Optical Waveguides (ARROW) have been used. On the basis of a quad beam accelerometer design, a sensing waveguide has been placed on the seismic mass. Its misalignment with the waveguides located at the frame allows measuring the acceleration. The mechanical structure has been designed so as to have a span of 2 μm, that should provide with a sensitivity of 4.6 dB/g. Reference waveguides measured by end-fire coupling have low radiation and insertion losses (0.3 and 2.5 dB, respectively). High insertion losses are observed due to imperfections in polishing when V-grooves with glass anodic bonding are used. This fact causes the reduction of its sensibility to 2.3 dB/g.

Keywords: Accelerometer; MOEMS; Integrated optics; Technology

1. Introduction

To overcome the inherent problems of electrical-based accelerometers, as could be temperature dependence, low sensitivity and non-stable output under electromagnetic interference (EMI) [1], there has been several proposals of optical-based accelerometers, both using integrated optics [2] and fiber optics [3]. The complete immunity against EMI and the possibility of having the light sources far from the device also makes them extremely useful in explosive atmospheres or where a strong electromagnetic field is present.

Up to date, the most common light guiding structures used on optical accelerometers have a high refractive index etched layer (frequently silicon nitride) in a cantilever configuration [4]. Although they could be considered as optimum for MOEMS applications, it has to be noted that these waveguides normally have thicknesses around 0.2 μm. If it is taken into account that a standard monomode optical fiber has a 4 μm core, the high difference between the cross-section of both structures is the main responsible of the high insertion losses (>20 dB) of these waveguides in the visible range when light is inserted by end-fire coupling.

In order to overcome the high insertion losses of the high step-index waveguides it is necessary to obtain core dimensions similar to that of the single mode fiber optics. To our knowledge, it is not possible to obtain, by conventional clean room deposition techniques, such thicknesses of silicon nitride films due to the mechanical stresses, which cause the layer to crack if its thick exceeds from 0.6 μm. Other materials, for example silicon oxide, can be deposited with the required thickness. However, working with TIR waveguides with a small refractive index difference between the core and the surrounding layers requires thick surrounding layers in order to avoid that the evanescent field reaches the silicon substrate.

An alternative approach that allows obtaining waveguides with core comparable to that of the fiber optics are the ARROW structures, the configuration of which is shown in Fig. 1. They have received recently much attention due to its interesting properties [5]. Guiding in these waveguides is achieved via the Fabry Perot interferometer placed beneath the core. With a fixed core thickness (d_c) and refractive indexes of the core and the two cladding layers (n_c, n_1 and n_2, respectively), there exist some values for the first and second cladding layers (d_1 and d_2) where a ultra-high reflection (>99.96%) at the core-1st cladding boundary is observed for the TE_0. At the upper core-air boundary, the guiding is caused by standard TIR. Generally, the modes of

* Corresponding author. Tel.: +34-93-594-7700; fax: +34-93-580-1496.
E-mail address: andreu.llobera@cnm.es (A. Llobera).

0924-4247/$ – see front matter
doi:10.1016/j.sna.2003.10.053

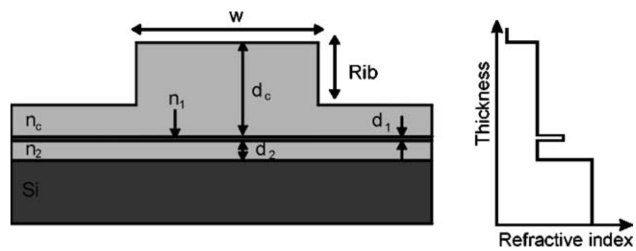

Fig. 1. Standard configuration and refractive index profile of ARROW structures. The darker the gray, the higher the refractive index is.

these structures are leaky modes since all of them present losses. Nevertheless, if the antiresonant pair is properly configured, theoretical losses for the fundamental mode are as low as 0.08 dB/cm. On the contrary, higher order modes are filtered out since the antiresonant layers are not properly sintonized. Hence, this structure has monomode behavior for core thickness of the same size as the fiber optics, minimizing the insertion losses.

2. Design and simulation

The basic configuration of the accelerometer is presented in Fig. 2. The quad beam mechanical structure [6], as compared with the cantilever configuration, presents the clear advantage to have a flat displacement in the sensing direction (*y*-axis). Thence, the misalignment between the waveguides located at the frame and at the mass is only produced in one axis. In order to collect as much light power as possible, the beam broadening in each cut has been compensated by making the waveguides progressively wider in the *x*-axis (14, 30 and 50 μm the input, the sensing and the output waveguide, respectively). Nevertheless, the most important broadening is produced in the *y*-axis, and it has been considered by reducing the step distance to 24 μm. If the mass was broken, the configuration will be an input and output aligned waveguides distanced a length slightly larger than the seismic mass (4000 μm). Thence, extremely high losses should be obtained, conferring an auto-test system. Finally, the proposed accelerometer is a combination of two opposite technologies: the micromechanized, which requires single layers in order not to have bending due to differences in the thermal expansion coefficients, and the ARROW, which is a multilayered structure with high mechanical stresses. The agreement with both technologies can be achieved if the waveguides are only placed in the bulk parts of the accelerometer (i.e., in the middle of the seismic mass) and maintaining the most sensitive silicon parts of the accelerometer (the beams and the corners) free of any other material than silicon.

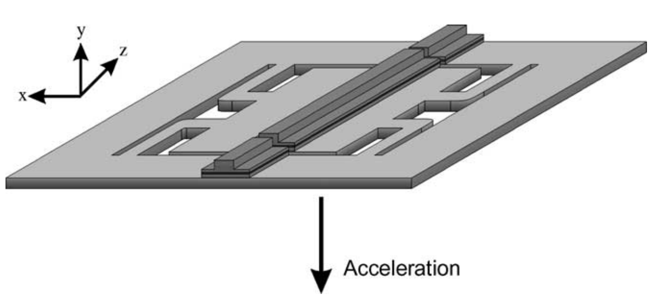

Fig. 2. Scheme of the quad beam optical accelerometer design.

Optical simulations of the device losses as a function of the seismic mass displacement were done using the finite difference method (FDM) [7] together with the beam propagation method (BPM) [8]. Although Si_3N_4/SiO_2-based ARROW structures had previously been studied [9], it was necessary to analyze the effects of the misalignment between the waveguide on the seismic mass and the waveguides located at the frame.

Fig. 3 shows a lateral view of the light intensity propagating through the device. When all the waveguides are aligned (a), a minimum loss is presented. As the seismic mass starts moving, the misalignment causes a sharp increase of the losses (b) and (c). If the seismic mass is broken, that is, if there is no intermediate waveguide, losses reach its maximum, as observed in Fig. 3d. Hence, it was possible to define the two linear regions shown in Fig. 4, with an optical sensitivity of 4.6 dB/g into which the losses are proportional to the misalignment. In order to confirm the behavior predicted by simulations, the span of the accelerometer was fixed to 2 μm.

Once the working region was established, the mechanical properties were chosen so as to fulfill the optical requirements. Mechanical optimization of the structure

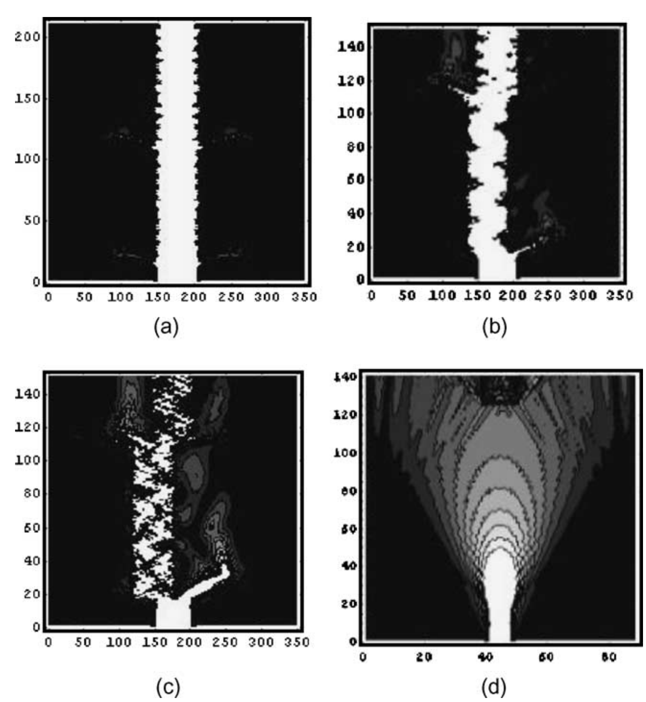

Fig. 3. Optical simulation of the waveguide misalignment: (a) no misalignment, (b) 30% misalignment, (c) 60% misalignment and (d) without intermediate waveguide.

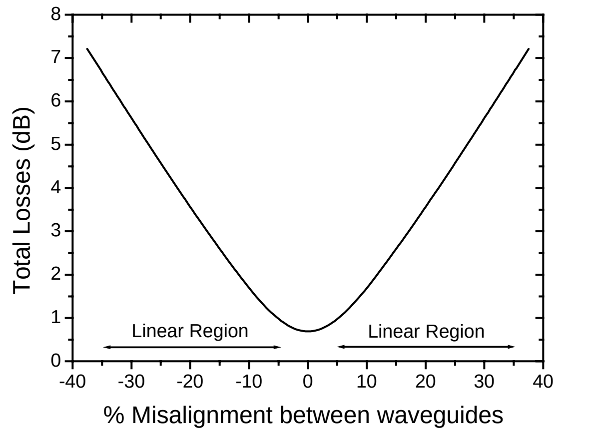

Fig. 4. Losses as a function of the waveguide misalignment, showing the two large linear regions.

Table 1
Maximum displacement of the mass and misalignment between the waveguides on the frame and on the mass versus the three directions of the acceleration

Acceleration (1*g*)	Maximum mass displacement (μm)	Waveguides misalignment (μm)
Y-direction	1.050	1.050
X-direction	0.105	0
Z-direction	0.202	0.202

was done via the finite element method (FEM) using ANSYS 5.7. The beams of the accelerometer were designed to have a mechanical sensitivity of 1 μm/g. Thence, the analytical total losses at maximum range are 4.6 dB. The cross-sensitivities were also simulated and are presented in Table 1. It can be observed that although misalignment obtained matched with the expected mass movement, there exists significant cross-acceleration effects: the mass displacement is 0.202 μm/g for *z*-accelerations and 0.105 for *x*-accelerations. It has to be noted, however, that since the waveguide is located at the center of the seismic mass, movements on the *x*-direction would not affect its relative position. Thus, the device is completely insensitive to accelerations in the *x*-direction. Modal simulations were done to estimate the natural frequency of the devices. The simulated frequency for the lowest mode is 489 Hz.

3. Fabrication

Accelerometers were fabricated on a N type, (1 0 0) oriented, 450 μm thick Bond and Etch Back Silicon On Insulator (BESOI) wafers from ShinEtsu [10]. Thickness of the upper silicon and buried silicon layers are 15 and 2 μm, respectively. In these substrates is grown the second cladding layer (2 μm of silicon dioxide), obtained by wet oxidation at 1000 °C. First cladding is a 0.38 μm LPCVD silicon nitride obtained at 700 °C. Core layer consists in

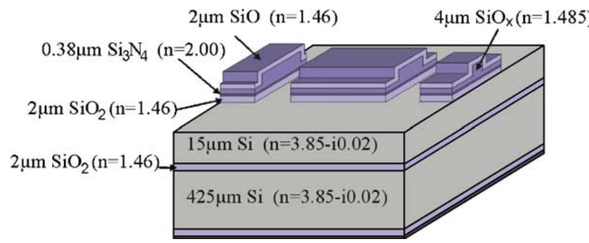

Fig. 5. Wafer status after ARROW waveguide definition.

a PECVD-deposited silicon oxide, with refractive index $n = 1.485$. This layer is 3.5 μm etched using RIE in order to assure cross-section confinement. Finally, a 2 μm PECVD silicon oxide layer was deposited over the waveguides so as to protect them against dust or scratches that would cause an increase of the device losses, not due to the working principle, but to defects in its guiding structures.

The following step was the complete removal of all the ARROW layers from the substrate except where the rib has been defined (Fig. 5). Concretely, the technological process mask were designed so as to leave the ARROW structure only at 100 μm in distance from the rib.

Layer thicknesses to be etched were significantly high. This forces using aluminum as a mask material. Micromechanical structure was defined in two steps: firstly, an anisotropic etching in KOH at the back of the wafer provided the three-dimensional structure. Anisotropic etching was done in KOH. As compared to TMAH, the former has a higher selectivity on etching (1 0 0) and (1 1 1) planes (which provides with a better accuracy on obtaining the expected geometry) and a minor lateral etching (which allows defining smaller convex corner compensation structures). Moreover, due to the KOH selectivity, either in the (1 1 1) and silicon oxide etching rate, the etching is automatically stopped at (1 1 1) planes and when the buried silicon oxide layer is reached (Fig. 6). Once the wafer was defined at the back, a photolithographic step with thick (6 μm) photore-

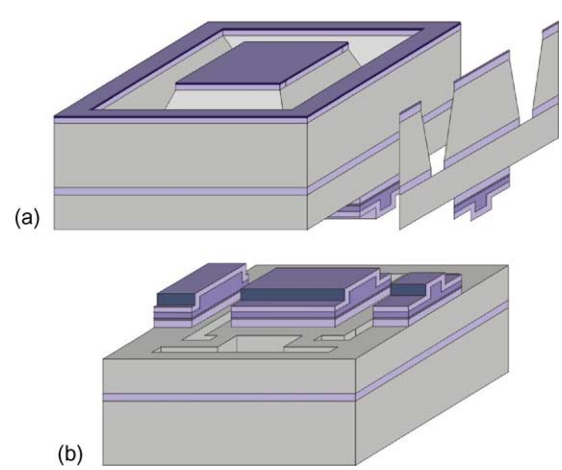

Fig. 6. Wafer status: (a) after anisotropic etching from the backside and (b) after dry etching from the front side to release the structure.

(a)

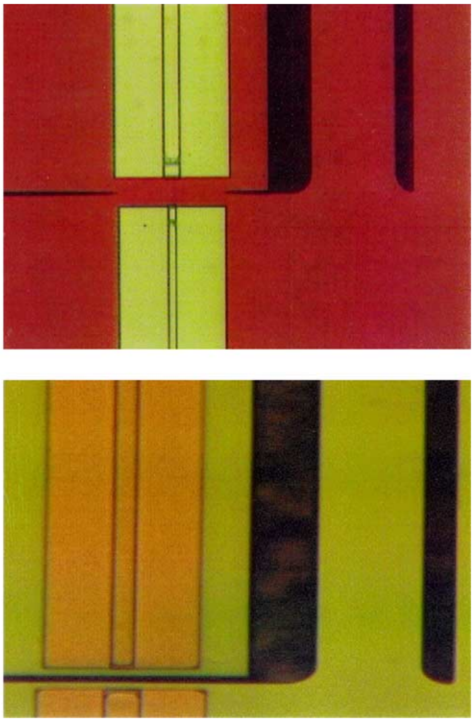

(b)

Fig. 7. Shadow mask problem during the dry etching: (a) with standard photolithographic step and (b) after overexposition.

sist, followed by a dry etching RIE at the front released the accelerometer.

As can be observed in Fig. 7a, the shadowing mask effect appeared during the dry etching process, which prevented from releasing the structure. This inappropriate photolithographic step can be understood if it is taken into account that there was a high step (8.38 μm) between the silicon substrate and the passivation layer (that forces using a thick photoresist to cover it). Thence, in order to have a good definition of the seismic mass on the front, it was necessary to do an overexposition. As can be observed in Fig. 7b, results obtained were clearly satisfactory and seismic mass was liberated from the frame.

Although the accelerometer fabrication could be considered as finished at this point, the devices were extremely fragile and cracked easily. For this reason a glass wafer (Pyrex #7740) previously mechanized was bonded on the back of the silicon wafer, as shown in Fig. 8.

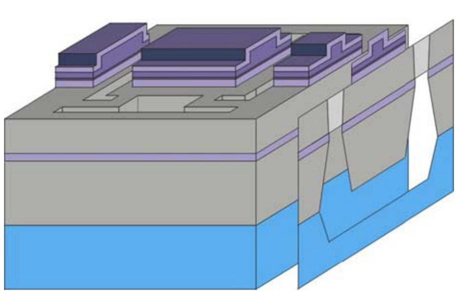

Fig. 8. Wafer status after anodic bonding to a glass wafer.

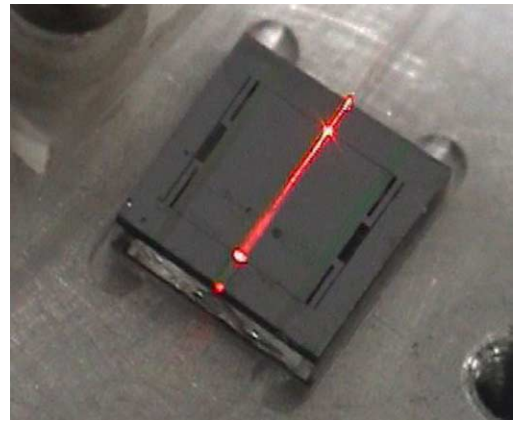

Fig. 9. First measurements of the accelerometer with non-stacked input and output fiber optics.

4. Characterization

Reference waveguides were measured by end-fire coupling so as to determine the radiation and insertion losses at $\lambda = 633$ nm and provided with results of 0.3 dB/cm and 2.5 dB, respectively. First measurements done as shown in Fig. 9 with the optical accelerometer showed losses of 6.8 dB. However, both the input and output fiber optics were able to move freely. Then, it was not possible to do an accurate characterization of the device, since it was the uncertainty whether the measured losses were due to the seismic mass displacement and not to or to the misalignment between the input/output fiber optics and the device. Placing the fiber optics in V-groove made of silicon solved this problem. The accelerometer was firstly fixed to a mechanized aluminum piece that has a slight minor length than the accelerometers. V-grooves were then able to move in the three axis until they were correctly aligned, being then glued. When the glue dried, two self-aligned pieces were placed underneath the V-grooves so as to provide the whole structure with robustness.

Light injection by end-fire coupling requires completely flat facets in order to minimize insertion losses. Although it is relatively simple to obtain high-quality facets by silicon polishing, results are not so optimal when a silicon-glass substrate has to be polished. The difference on the stiffness between both materials causes to have a tapered facets and defects on it. This is the main reason why after stacking the accelerometer and the V-grooves, losses increased until 18.3 dB, which is two times higher than the value obtained by simulations. Nevertheless, power obtained at the output still allows an appropriate optical characterization.

Accelerometer response as a function of the gravitational field was measured using a Ferris wheel that has a controlled angular movement in such a way that the acceleration applied to the device was the projection of this magnitude to the sensible axis of the device. Results can be seen in Fig. 10. As can be observed, the expected periodical response as a function of the angle is obtained. It has to be noted that

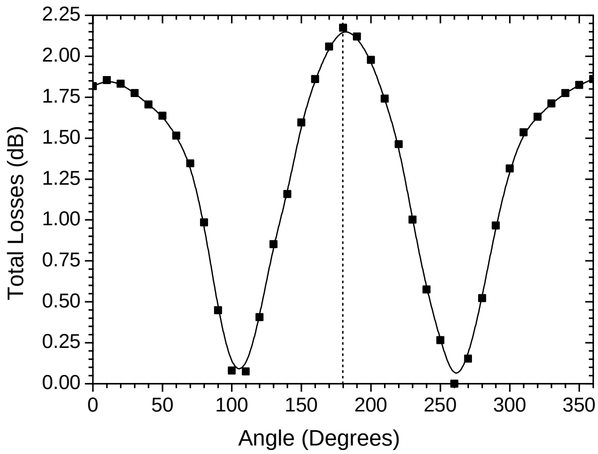

Fig. 10. Accelerometer output intensity as function of the gravity field tilt.

losses shown in this figure have been re-ranged, being the zero fixed for the maximum power output. This has been done so as to determine the optical accelerometer sensitivity. It can be observed that minimum losses are not obtained at 90° and 270°, which provide with an acceleration of 0 g, but have a slight displacement to 100° and 260°. This value corresponds to a small misalignment between waveguides of 0.18 μm.

Although the behavior between the two minimum losses presents a high linearity around the point of minimum losses, it can be observed that seismic mass displacement does not cause symmetrical power variations, since at the region between 0° and 90° (and also between 270° and 360°) a tail is observed in the experimental data. This fact can be understood if it is taken into account that waveguides have passivation that has the same properties as the standard passivation in fiber optics. When the accelerometer suffers from large negative values of the acceleration, light is partially injected to the passivation, causing a decrease of the losses. This fact is not observed at positive acceleration values since the light injected in the second cladding is fastly absorbed by the silicon of the seismic mass.

5. Conclusions

An optical accelerometer based on antiresonant waveguides has been designed so as to have an optical sensitivity of 4.6 dB/g. The fabrication process using BESOI wafers has proved its viability and reference waveguides presented the expected low radiation and insertion losses (0.3 dB/cm and 2.5 dB) at the working wavelength. Although inappropriate polishing of the V-grooves have caused a significant increase of the insertion losses, static measurements done have provided with the expected response to the acceleration. Measurements done have proved that waveguides only are 0.18 μm misaligned, with a highly lineal but asymmetric response, due to the passivation.

Acknowledgements

A. Llobera thanks the Generalitat de Catalunya (Catalan Council) for grant no. 2001-TDOC-00008.

References

[1] N. Yazdi, F. Ayazi, K. Najafi, Micromachined inertial sensors, Proc. IEEE 86 (8) (1998) 1640–1659.

[2] J.M. López-Higuera, P. Mottier, A. Cobo, E. Ollier, M.A. Morante, C. Chabrol, et al., Optical fiber and integrated optics accelerometers for real time vibration monitoring in harsh environments: in-lab and in-field characterization, in: Proceedings of the EWOFS'98 (SPIE), vol. 3483, 1998, pp. 223–226.

[3] J. Kalenik, R. Pajak, A cantilever optical-fiber accelerometer, Sens. Actuat. A 68 (1998) 350–355.

[4] K.E. Burcham, G.N. de Brabander, J.T. Boyd, Micromachined silicon cantilever beam accelerometer incorporating an integrated optical waveguide, in: Proceedings of the SPIE 1793 Integrated Optics and Microstructures, 1992, pp. 12–18.

[5] T. Baba, Y. Kokubun, Dispersion and radiation loss characteristics of antiresonant reflecting optical waveguides—numerical results and analytical expressions, IEEE J. Quant. Electron. 28 (7) (1992) 1689–1700.

[6] T. Tschan, N. de Rooij, A. Bezinge, Analytical and FEM modelling of piezoresistive silicon accelerometers: predictions and limitations compared to experiments, Sens. Mater. 4 (1992) 189–203.

[7] C.M. Kim, R.V. Ramaswamy, Modelling of graded-index channel waveguides using nonuniform finite difference method, J. Light. Technol. 7 (10) (1989) 1581–1589.

[8] Y. Chung, N. Dagli, Analysis of Z-invariant and Z-variant semiconductor rib waveguides by explicit finite difference beam propagation method with nonuniform mesh configuration, IEEE J. Quant. Electron. 27 (10) (1991) 2296–2305.

[9] I. Garcés, F. Villuendas, J.A. Vallés, C. Domínguez, M. Moreno, Analysis of leakage properties and guiding conditions of rib antiresonant reflecting optical waveguides, J. Light. Technol. 14 (5) (1996) 798–805.

[10] J.A. Plaza, J. Esteve, E. Lora-Tamayo, Simple technology for bulk accelerometer based on bond and etch back silicon on insulator wafers, Sens. Actuat. A 68 (1998) 299–302.

Biographies

A. Llobera was born in Barcelona, Spain, in 1974. He received his degree and PhD in physics from the Universitat Autònoma de Barcelona in 1997 and 2002, respectively. He is currently holding a Postdoctoral position at the Institut für Mikrotechnik, belonging to the Technishe Universität Braunschweig, Germany. His research activities include the design, simulation and characterization of integrated optical devices and the development of new materials for optoelectronics.

J.A. Plaza was born in Cerdanyola del Vallés, Barcelona, Spain, in 1968. He received his physicist degree and PhD degree in electronics engineering from the Autonomous University of Barcelona (1992, 1997). Currently he is working in the Department of Silicon Technologies and Microsystems of the Institut de Microelectrònica de Barcelona (IMB-CNM, CSIC) in Bellaterra, Spain. His research focuses on the design, fabrication and characterization of accelerometers, pressure sensors, anodic bonding and microfluidics.

I. Salinas was born in Pamplona, Navarra, Spain, in 1973. He received his MS degree in physics in 1996 and PhD in 2003 from the Sciences

Faculty at the University of Zaragoza, Spain. He holds currently an academic position in the Electrical Engineering and Communications Department, University of Zaragoza, and is a member of the Instituto de Investigación en Ingeniería de Aragón (I3A). His main research interests are integrated optics, WDM optical networking and optical instrumentation.

J. Berganzo was born in Vitoria, Spain, in 1965. He received his BS degree in electronic engineering from the Mondragon University and MS degree in electric engineering from the Lausanne's Swiss Federal Institute of Technology (1990). Currently he is working in the Microsystems Area of Ikerlan in Mondragon, Spain. His research focuses on the design, fabrication and characterization of mechanical sensors, microfluidics and packaging technologies.

J. Garcia was born in San Sebastián, Spain, in 1968. He received his MS and PhD degree in engineering from the University of Navarra (1992, 1997). Currently he is working in the Department of Microsystems of Ikerlan in Mondragon, Spain. His research focuses on the simulation, design, fabrication and characterization of pressure sensors, electroplating and micro-optics.

J. Esteve was born in Parets del Vallés, Barcelona, Spain, in 1961. He received his PhD degree in physical electronics from the University of Barcelona in 1988. In 1990 he joined the CNM's Department of Silicon Technologies and Microsystems as a Senior Research Scientist. His areas of interest include silicon micromachining technologies and their application to integrated sensors and actuators.

C. Domínguez received his BS, MS, and PhD degrees in chemistry from the Universidad Complutense of Madrid, Spain, in 1980, and 1985, respectively. He became a member of the scientific staff at the Institut de Microelectrònica de Barcelona (IMB-CNM, CSIC) in 1986. Since 1991 he has been a Senior Scientific Researcher at IMB-CNM, CSIC. He is involved in chemical vapor deposition processes and wet and dry etch processes. Currently he is working on the development of an integrated optical technology based on silicon for sensors and broad-band telecommunications applications.